Available online at www.sciencedirect.com
SCIENCE DIRECT®

Journal of Catalysis 228 (2004) 225–233

JOURNAL OF CATALYSIS

www.elsevier.com/locate/jcat

FTIR and reaction studies of the acylation of anisole with acetic anhydride over supported HPA catalysts

B. Bachiller-Baeza[1], J.A. Anderson[2,*]

Surface Chemistry and Catalysis Group, Division of Physical and Inorganic Chemistry, The University, Dundee DD1 4HN, Scotland, UK

Received 1 July 2004; revised 4 August 2004; accepted 4 August 2004

Abstract

The behaviours of two heteropoly acid (HPA) catalysts, one supported on a commercial silica and the other on a silica–zirconia mixed oxide, were compared in the acylation of anisole with acetic anhydride. Both supported catalysts and the latter support, but not the silica, were active for the reaction, although all underwent a deactivation process before achieving complete conversion of anisole to *p*-methoxyacetophenone. The greatest yield to *p*-methoxyacetophenone was obtained for HPA/SiO_2 while the extent of deactivation was in the order HPA/SiO_2–ZrO_2 > SiO_2–ZrO_2 > HPA/SiO_2. Although acetate species accumulated on the SiO_2–ZrO_2 and HPA/SiO_2–ZrO_2 catalysts during the reaction, these species are not thought to play a role in the deactivation process. The relative extent of deactivation was consistent with the calculated ratios of adsorption coefficients which determine the strength of adsorption of product to that of anisole and indicate that product inhibition is greatest in the case of HPA/SiO_2–ZrO_2. Calculated absorption coefficients for pyridine adsorbed on the samples failed to distinguish between the nature of the HPA species dispersed on the two different supports.

Keywords: Supported heteropoly acid; Anisole; Acylation; Silica–zirconia; Acid site densities

1. Introduction

Friedel–Crafts acylation to produce substituted aromatic ketones is an important key step in the production of intermediates for use in the pharmaceutical, cosmetics, and speciality chemicals industries [1]. The present industrial method used to synthesize these ketones applies homogeneous Lewis acid-type catalysts (anhydrous metal halides, $AlCl_3$, $FeCl_3$) and acyl halides as acylating agents. The overall process produces a significant amount of undesirable products and destroys the catalyst. The use of solid acids as catalysts represents an attractive alternative with economic and environmental advantages. Among these materials, zeolites, which combine acidic properties with shape selectivity, and modified metal oxides are the most widely studied [2,3]. As a result of their strong and well-documented acid properties, heteropoly acids would also appear to be a potential solid catalyst for this reaction. Supported heteropoly acids present a greater number of surface acid sites than their bulk counterparts which favours their use as heterogeneous catalysts. The acidity depends mainly on the support and loading, supports such as SiO_2 and carbons being the most widely examined as they are inert to the heteropoly acid [4,5]. In general, the acidity at low loadings is weaker and less uniform than for the bulk solid, and some decomposition of the heteropoly acid may be observed [6]. As the loadings increases, the acid strength also increases. The basicity of the support is thought to be one of the factors which determines the activity of supported heteropolyacid catalysts in acid–base-type reactions [7].

One drawback that limits the use of the solid acids in commercial Friedel–Crafts acylation processes is the signif-

---

[*] Corresponding author.
E-mail address: j.anderson@abdn.ac.uk (J.A. Anderson).

[1] Present address: Inst. de Catálisis y Petroleoquímica (CSIC), c/Marie Curie s/n, Campus de Cantoblanco, 28049, Madrid, Spain.

[2] Present address: Surface Chemistry and Catalysis Group, Department Chemistry, Kings College, University of Aberdeen, Old Aberdeen AB24 3UE, Scotland, UK.

doi:10.1016/j.jcat.2004.08.010

icant deactivation of these systems during use in reaction. The deactivation phenomena may result from product inhibition or competitive adsorption of the reactants, but can be also due to coke deposition. In zeolite catalysts, heavy reaction products within the pores and on the outer surface of the crystallites seem to be responsible for the apparent deactivation [8,9].

In this paper, the behaviours of two supported heteropoly acid catalysts are compared in the acylation of anisole with acetic anhydride. The catalysts were prepared using supports with very different acidic properties; a commercial silica with no acidic properties and a silica–zirconia mixed oxide which exhibits both Brønsted and Lewis acidity. To investigate the possible influence of the type of acidity in the mechanism of deactivation, a spectroscopic study of the interactions of the acylating agent and the reactant with the acid sites of the catalysts has been performed.

2. Experimental

The HPA-supported catalysts, with a 10% loading, were prepared by impregnating the support previously dispersed in water, with an aqueous solution of the Keggin-type heteropoly acid ($H_3PW_{12}O_4 \cdot H_2O$, Aldrich). The dispersion was stirred for 2 h and then evaporated to dryness, and the resulting solid dried overnight at 343 K. Two supports were studied: a commercial silica (EP 10) and a silica–zirconia mixed oxide prepared via a sol–gel technique as described previously [10]. Briefly, the silica–zirconia support was synthesized from a tetraethylorthosilicate (TEOS) solution prehydrolysed for 2 h, which was combined with a zirconium tetrapropoxide solution in propanol using nitric acid as hydrolysis catalyst. The gel obtained was subjected to a solvent-exchange process by refluxing in ethyl acetate and the material was dried under supercritical CO_2. Finally, the solid was calcined for 5 h in a flow of air at 873 K. The BET areas of the resulting supports and supported catalysts were 300 (SiO_2), 194 (HPA/SiO_2), 317 (SiZr), and 168 $m^2\,g^{-1}$ (HPA/SiZr).

Acylation of anisole was carried out at 363 K in the liquid phase under an atmosphere of N_2 in a 100-ml glass reactor equipped with a condenser and magnetic stirrer. The catalysts (150 to 170 mg) were pretreated in vacuum at 423 K for 1.5 h and then transferred to the reaction vessel where the mixture of anisole and acetic anhydride was kept at the reaction temperature. An anisole to acetic anhydride ratio of 10:1 was chosen to allow data to be directly compared with published results. Samples were taken periodically and analysed by gas chromatography using dodecane as an internal standard.

Determination of the surface acid site densities was carried out by combining thermogravimetric and infrared spectroscopic techniques [11]. Thermogravimetric analyses were carried out using a PC-controlled CI microbalance attached to a conventional vacuum line and monitoring the mass at 3-s intervals throughout the experiment. The sequence of treatments applied to the samples was outgassing at 573 K for 2 h, exposure to 1 Torr pyridine, and cooling to 373 K, further introduction of a 0.5 Torr pulse of pyridine and allowing for equilibration over 30 min, and then heating under vacuum to 423 K for 1 h and finally to 473 K for another 1 h. The infrared experiments were carried out on a pressed sample treated in the same fashion as for the thermogravimetric measurements. The spectra were recorded after the evacuation at 573 K and after exposure to pyridine and subsequent outgassing at 423 and 473 K. Surface densities of both acid sites were calculated by applying the Brønsted and Lewis absorption coefficients determined by combination of the mass of pyridine retained at the two temperatures and the integrated area underneath the bands due to the pyridine adsorbed at the Brønsted (1540 cm^{-1}) and Lewis (1450 cm^{-1}) acid sites as previously described [11,12].

IR spectra for anisole and acetic anhydride coadsorption at increasing vapour pressures were recorded on a Perkin–Elmer 1710 FTIR spectrometer at 4 cm^{-1} resolution and as an average of 50 scans. The samples were pressed into a 16-mm-diameter disks and evacuated at 423 K for 1.5 h in a quartz cell connected to a conventional vacuum line. The two compounds were degassed by repeating a freeze-and-thaw cycle and used without further purification.

3. Results

3.1. Reaction of acylation of anisole

The heteropolyacid-supported catalysts were studied in the reaction of anisole with acetic anhydride at 363 K. Although *o*-methoxyacetophenone was detected, the main product of the reaction was *p*-methoxyacetophenone, with selectivities greater than 97%. Fig. 1 shows the evolution of *p*-MAP yield with time in reaction for SiZr, HPA/SiO_2,

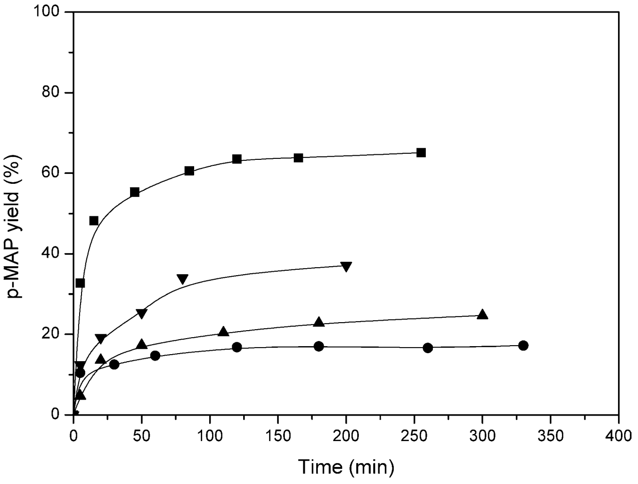

Fig. 1. Yield of *p*-methoxyacetophenone in the acylation of anisole with acetic anhydride at 363 K for: (■) HPA/SiO_2, (▲) SiZr, and (●) HPA/SiZr catalysts and at 333 K for (▼) HPA/SiO_2.

and HPA/SiZr catalysts. A clear deactivation occurred for all the samples as indicated by reaching a plateau between 50 and 100 min before attaining full conversion. This deactivation has been attributed in part to the retention of the reaction product, *p*-MAP, adsorbed on the acid sites of the catalysts, thereby hindering the adsorption of anisole [9,13]. The maximum yield to *p*-MAP was 65%, obtained with the system HPA/SiO_2 at 363 K and this decreased to 37% when the reaction was performed at 333 K. These results compare well with other previously reported values for heteropoly acids supported on silica, where the yield varied in the range 61–98% depending on the HPA content, reaction temperature, and anisole/acetic anhydride ratio [13]. On the other hand, both SiZr and HPA/SiZr samples gave comparatively low yields of around 20%, somewhat less than the silica-supported sample. It is important to note that for SiZr and HPA/SiZr a difference was observed between the conversion and the yield of MPA, which might indicate that some consumption of AcAn took place, resulting in deposits on the catalyst surface.

3.2. FTIR

3.2.1. Surface hydroxylation

Spectra in the hydroxyl stretching region for samples evacuated at 523 K are displayed in Fig. 2. All the samples showed a narrow band at ca. 3750 cm^{-1} assigned to isolated silanols on the silica support and to the silica component of the silica–zirconia aerogel. The broader feature centred at ca. 3550 cm^{-1} is associated with different hydrogen-bonded surface hydroxyls and adsorbed water. The latter features were much more prevalent for the HPA-containing samples (Fig. 2, b and c) than for the SiZr support alone (Fig. 2, a), suggesting that strongly retained water molecules were associated with the heteropolyacid component.

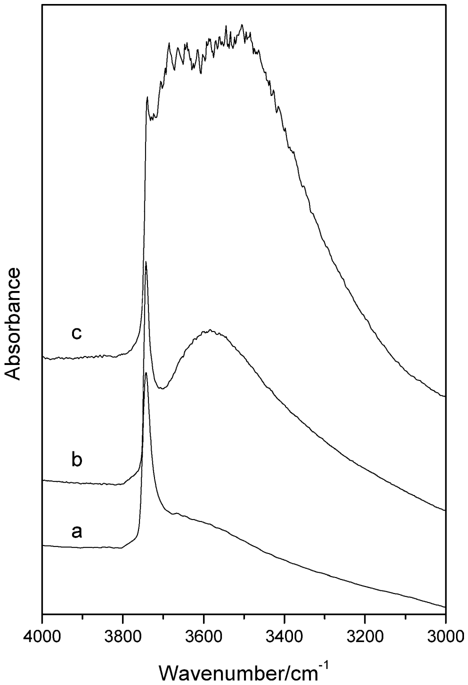

Fig. 2. FTIR spectra for (a) SiZr, (b) HPA/SiZr, and (c) HPA/SiO_2 after evacuation at 523 K.

3.2.2. Pyridine adsorption

In Fig. 3, spectra are presented of pyridine adsorption on samples HPA/SiO_2, SiZr, and HPA/SiZr. The spectra revealed bands characteristic of coordinative adsorption of pyridine on Lewis acid sites (1610 and 1450 cm^{-1}) and of the pyridinium ion formed by interaction with Brønsted acid sites (1640 and 1540 cm^{-1}). Both types of adsorbed species contribute to the band at 1490 cm^{-1}. However, the exact nature of the spectra differed from sample to sample. The spectra for HPA/SiO_2 showed only bands ascribed to the adsorption of pyridine on Brønsted acid sites. The dispersion on silica of the heteropoly acid, which is known as a material with characteristic Brønsted acid properties, generates Brønsted acid sites on the surface. The support silica did not show features of either Brønsted or Lewis acidity. Consistent with previous studies [14,15] the SiZr sample showed evidence for the presence of both Lewis and Brønsted acid sites. It is well established that the addition of zirconia to silica leads to the formation of Lewis and Brønsted acid sites even though the latter are absent on the component oxides [14], and that the density and strength of the Lewis and Brønsted acid sites created depend on different factors, i.e., the Si/Zr ratio, preparation conditions, etc. [15]. The HPA/SiZr exhibited a more pronounced band at 1540 cm^{-1} than for the

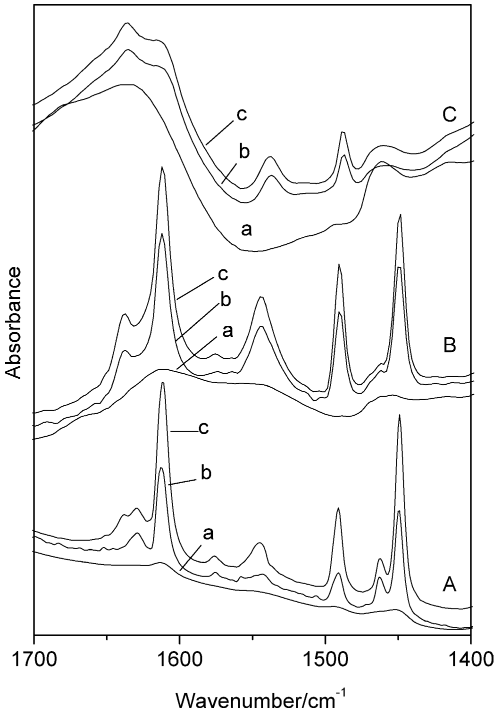

Fig. 3. FTIR spectra of (A) SiZr, (B) HPA/SiZr, and (C) HPA/SiO_2 after (a) outgassing at 523 K, and adsorption of pyridine followed by evacuation at (b) 423 and (c) 473 K.

SiZr support alone, implying a greater number of Brønsted sites in this sample. Additionally, on comparing the spectra of SiZr and HPA/SiZr samples after outgassing at 423 and 473 K, the integrated band area at 1540 cm^{-1} decreased to a greater extent for the former. This suggests that a relatively greater proportion of base molecules remained adsorbed on the Brønsted sites after outgassing at 473 K for HPA/SiZr, and consequently that the strength of the majority of the Brønsted acid sites on that sample were greater than for the support alone. It can be envisaged that two types Brønsted acid sites with different strength exist on HPA/SiZr, one associated with the HPA and the other due to the SiZr support. Moreover, it is well known that pyridine is absorbed into the bulk heteropolyacid and that this remains sorbed up till 573 K [16].

The total number of acid sites was determined thermogravimetrically, measuring the total amount of pyridine retained following outgassing at 423 and 473 K. Recently, an alternative method of obtaining this information was described for similar materials and involved temperature-programmed surface reaction of isopropanol [17]. The values shown in Table 1 indicate that the addition of HPA to SiO_2 creates a certain number of acid sites, which, in accordance with the FTIR spectra of adsorbed pyridine, are only of the Brønsted acid type. By comparison with the SiZr support, the addition of HPA to SiZr increased the number of acid sites per gram of the solid. The amount of base retained after 423 K outgassing for HPA/SiZr was greater than for HPA/SiO_2 and in fact corresponded to the sum of the amount of base adsorbed on the SiZr support, and on the HPA/SiO_2. This was not the case when samples were compared on the basis of pyridine retained following outgassing at 473 K, suggesting that the strength of available sites on the HPA/SiZr were not identical to those present on the individual components. If the number of base molecules retained at 423 K is evaluated per unit of HPA, the HPA/SiO_2 gave a value of approximately 3, which corresponds with the theoretical number of molecules needed to neutralize the polyanion [4], whereas the HPA/SiZr gave a value of 8. These results again indicate that adsorption of pyridine for the latter sample takes place not only on the Brønsted acid sites of the HPA, but also on the Brønsted and Lewis sites of the SiZr support. This value would clearly be reduced if only the base molecules adsorbed at Brønsted acid sites (value = 4) are considered and further reduced (value = 1) when the number of molecules adsorbed on Brønsted acid sites of the support is subtracted (see later following calculation of the densities using molar absorption coefficients). After heating and evacuating at 473 K, the number of retained molecules decreased for both HPA/SiO_2 and HPA/SiZr, consistent with the qualitative observations made in the FTIR spectra (Fig. 3).

The molar absorption coefficients for pyridine adsorbed at Brønsted and Lewis acid sites (Table 1) were determined by combining the IR and the gravimetric measurements [11]. The values obtained were 0.76 and 1.03 $cm\,\mu mol^{-1}$ for Brønsted and Lewis acid sites, respectively, on HPA/SiZr while for the SiZr support alone these were 0.53 and 1.78 $cm\,\mu mol^{-1}$ [12]. Sample HPA/SiO_2 showed only Brønsted acid sites and gave a coefficient of 0.80 $cm\,\mu mol^{-1}$. Similarity in the values for the molar absorption coefficient for the pyridinium ion on the HPA-containing samples gives credence to the calculated values. The acid site densities for HPA/SiO_2 and HPA/SiZr, i.e., molecules of pyridine retained per square nanometer, calculated from the molar absorption coefficients, are in line with the fact that heteropoly acids are mainly characterized by their high Brønsted acidity, and are again consistent qualitatively with the data deduced from the integrated areas of the infrared bands ascribed to adsorption on Brønsted and Lewis acid sites. The ratio of Brønsted to Lewis sites was 1.35 for SiZr but 1.1 for HPA/SiZr when compared after 423 K outgassing. This ratio fell to 0.83 for the SiZr after 473 K outgassing but was held at 1.1 for the HPA/SiZr, indicating that the strength of the Brønsted acid sites associated with the HPA was greater than that on the support. On the basis of base retained at both temperatures, the number of Brønsted acid sites on the HPA/SiZr is approximately equal to the sum of the sites on the HPA/SiO_2 plus the number on the SiZr support alone. However, the number of Lewis sites on the HPA/SiZr is not equal to the number on the SiZr support, suggesting that the additional Lewis sites may have been created on the HPA/SiZr by the process of HPA addition to the support. The process of sulphation of the SiZr support is known to

Table 1
Characterisation of the acid sites[a]

Sample	S_{BET} ($m^2\,g^{-1}$)	Total acid sites ($\mu mol_{Py}\,g^{-1}$)	Acid site per HPA unit ($mol_{Py}\,mol^{-1}_{HPA}$)	ε_{1540}[b]	ε_{1450}[b]	$n_{Brønsted}$[c]	n_{Lewis}[c]
HPA/SiO_2	194	95 (54)	2.8 (1.6)	0.80	–	0.294 (0.219)	0
SiZr	317	198 (111)	–	0.53	1.78	0.217 (0.096)	0.161 (0.116)
HPA/SiZr	257	288 (200)	8.3 (5.8)	0.76	1.03	0.540 (0.372)	0.494 (0.345)

[a] Based on mass of pyridine retained after evacuation at 423 and (473 K).
[b] IR molar absorption coefficient ($cm\,\mu mol^{-1}$).
[c] Numbers of acid sites per nm^2.

enhance Lewis acidity due to surface segregation of the zirconia component [18].

It is of interest to note that samples SiZr and HPA/SiZr showed a different number and distribution of acid sites (Lewis and Brønsted) and different acid strengths; both behave similarly in the reaction of acylation (Fig. 1). In addition, their catalytic behaviour differed greatly from the HPA/SiO_2, which presented only Brønsted acidity. The reaction studied is considered as a Brønsted acid-catalysed reaction with a mechanism that involves the formation of an acylium-type intermediate of the acylating agent [1,13]. Should no deactivation occur, a higher Brønsted acid site density should result in a higher yield of the product p-MAP when compared after a specific time of reaction. The marked differences in the yields obtained for HPA/SiO_2 and HPA/SiZr samples, despite the presence of the HPA, which should be dispersed over the support in both cases is very significant in terms of the relative deactivation of the two systems. This suggests the great effect of the nature of the support on the catalytic properties of the samples.

3.2.3. Coadsorption of anisole and acetic anhydride

The spectra in the range 1800–1300 cm^{-1} obtained for HPA/SiO_2 and HPA/SiZr after the subsequent adsorption of anisole and acetic anhydride (AcAn) from the vapour phase are shown in Figs. 4A and 4B.

The adsorption of anisole on HPA/SiO_2 (Fig. 4A, a) gave intense bands at 1600, 1500, 1470, and 1460 cm^{-1} that can be assigned to the aromatic C–C stretching modes. The addition of AcAn led to the decrease of the bands ascribed to anisole, indicating displacement of the adsorbed species by the second molecule. Moreover, new features appeared on the spectrum at 1758, 1716, and 1403 cm^{-1}, the latter possibly formed by contributions of different bands as shown later. The absorption bands at 1716 and 1403 cm^{-1} are assigned to physically adsorbed acetic acid in a dimeric state formed by decomposition of the AcAn probably due to the residual adsorbed water on the catalyst surface [19]. Note that evidence for the presence of retained water for the HPA-containing samples is provided by FTIR spectra of the samples after 523 K evacuation (Fig. 2, b and c). While the band at 1716 cm^{-1} is most likely due to the $\nu(C{=}O)$ stretching mode of the molecules bound to the surface OH groups by H bonding, the band at 1403 cm^{-1} can be assigned to the $\delta(CH_3)$ vibrations. In addition, the interaction of the lone electron pair of the carbonyl oxygen atom with the H resulted in a shift of the $\nu(O–H)$ band to lower frequencies (not shown). On the other hand, the band at 1758 cm^{-1} could be due to the $\nu(C{=}O)$ of a silyl ester species formed by dissociative adsorption of acetic acid, which would be associated with the asymmetric and symmetric $\delta(CH_3)$ modes (1435 and 1384 cm^{-1}) that contribute to the band at 1403 cm^{-1}. Further heating of the sample at 363 K, i.e., the temperature used in the acylation reaction experiments, did not result in any significant modification to the spectra, apart from an enhancement in the intensity of the shoulder at 1384 cm^{-1}. No clear evidence was obtained to indicate any reaction between the two different adsorbates on the catalyst. After evacuation at 298 K (Fig. 4A, d) only bands at 1734, 1605, 1435 (less intense), and 1383 cm^{-1} remained in the spectrum. This indicates that the silyl species, indicated by bands at 1734, 1435, and 1384 cm^{-1}, were very stable and strongly adsorbed on the surface, along with other deposits (1605 cm^{-1}) which were formed and retained after the coadsorption of anisole and AcAn.

The sample HPA/SiZr showed a similar spectrum as the HPA/SiO_2 catalyst for the adsorption of anisole (Fig. 4B, a), with bands at 1600, 1500, 1470, and 1460 cm^{-1}. However,

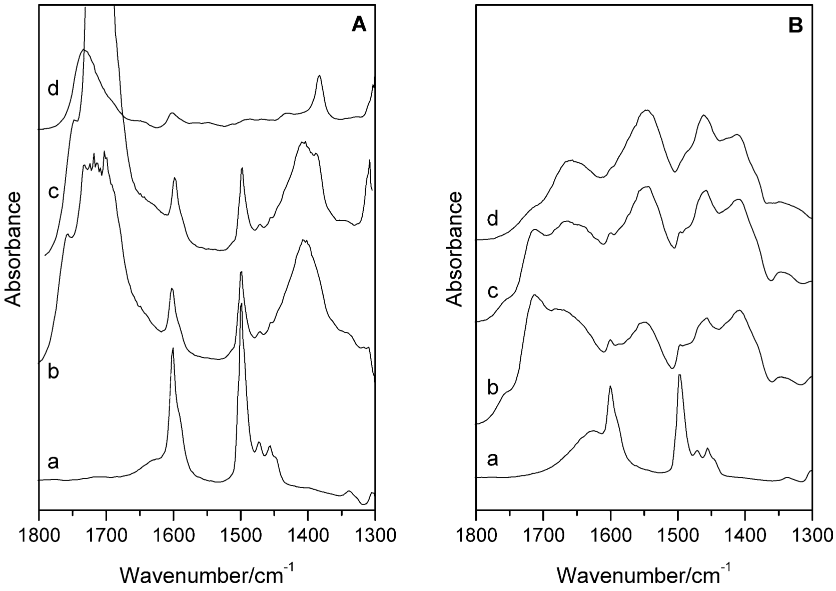

Fig. 4. FTIR spectra of (A) HPA/SiO_2 and (B) HPA/SiZr after (a) exposure to anisole and brief evacuation at 298 K, (b, c) addition of increasing pressures of acetic anhydride, and (d) heating at 363 K and evacuation.

following adsorption of AcAn the spectra of the two samples differed significantly. Apart from the peaks at 1601 and 1498 cm^{-1} that correspond to the residual adsorbed anisole and the shoulder at 1757 and the bands 1718 and 1410 cm^{-1} that can be assigned to silyl ester species and molecular adsorbed acetic acid, additional bands at 1654, 1550 and 1457 cm^{-1} were observed. The latter two features are characteristic of the antisymmetric and symmetric $\nu(COO^-)$ vibrations, respectively, of chemisorbed acetate species. Since the splitting of these frequencies is less than 150 cm^{-1}, it may be inferred that the acetate is in a bidentate configuration. The band at 1654 cm^{-1} may be associated to acyl species formed by reaction with Brønsted acid sites. Brief outgassing and heating to 363 K changed the relative intensity of the bands, but the positions remained constant. Subsequent evacuation (Fig. 4B, d) led to a spectra dominated by bands corresponding to acetate species (1550 and 1450 cm^{-1}) and acyl species (1650 and 1410 cm^{-1}). At this point it is important to note that the band at 3735 cm^{-1} (not shown), due to the silanol groups of the silica component of the mixed oxide, was depleted after the adsorption of anisole and briefly recovered after the final outgassing treatment. This observation confirms the participation of such OH groups in the adsorption of the reactant molecules but indicates that they are not consumed by the process. The same experiment, but performed by reversing the order of adsorption of the compounds, namely AcAn first and then anisole, gave a final spectrum identical to the one shown in Fig. 4B (d), which is an indication of the stronger adsorption of AcAn leading to formation of acetate species after the coadsorption of the two reactants on this catalyst. Furthermore, this experiment showed that acetates and acyl species are formed after exposing the catalyst to the AcAn, and that only after increasing the coverage are silyl species and molecularly adsorbed acetic acid observed. A band at 1831 cm^{-1} ascribed to the molecular anhydride was detected at the highest dosage of this adsorbate.

The concentration of the surface acetate species was estimated by calculating the integrated intensity of the acetate band at 1450 cm^{-1} and employing a molar absorption coefficient of 1.7×10^{-17} cm $molecule^{-1}$ [20]. Assuming these acetates are located exclusively on the zirconia component, then from the Si/Zr surface atomic ratio of 2.63 determined by XPS for the original support [18] and using the values of 20.0 and 8.1 $Å^2$ for the unit areas occupied by ZrO_2 and SiO_2, respectively, the density of acetates becomes 3.5 per square nanometer of exposed zirconia which equates to a coverage of 70% of the exposed zirconia.

3.2.4. Catalyst after reaction

Fig. 5 shows the spectra of the HPA/SiO_2 and HPA/SiZr samples which were recovered after the acylation of anisole with acetic anhydride at 363 K. The spectrum in the region of carbonyl stretching vibrations for the silica-supported heteropolyacid (Fig. 5A) presents bands at 1657, 1600, 1576, 1512, 1462, 1421, and 1364 cm^{-1}, originating from the adsorbates and other reaction products. After Soxhlet extraction in CH_2Cl_2 for 3 h, removal of species which had previously given the main bands at 1600, 1513, 1422, and 1364 cm^{-1} was observed, indicating successful extraction of the compounds retained by the catalyst, most likely the product *p*-methoxyacetophenone. The broad band at 1630 cm^{-1} is due to the bending vibration of the molecularly adsorbed water. Evacuation at room temperature under vacuum (Fig. 5A, c) led to the removal of water leaving bands at 1635, 1594, and 1503 cm^{-1} which correspond to hydrocarbonaceous deposits resulting from the polyacetylation of anisole and other monoacetylated deriv-

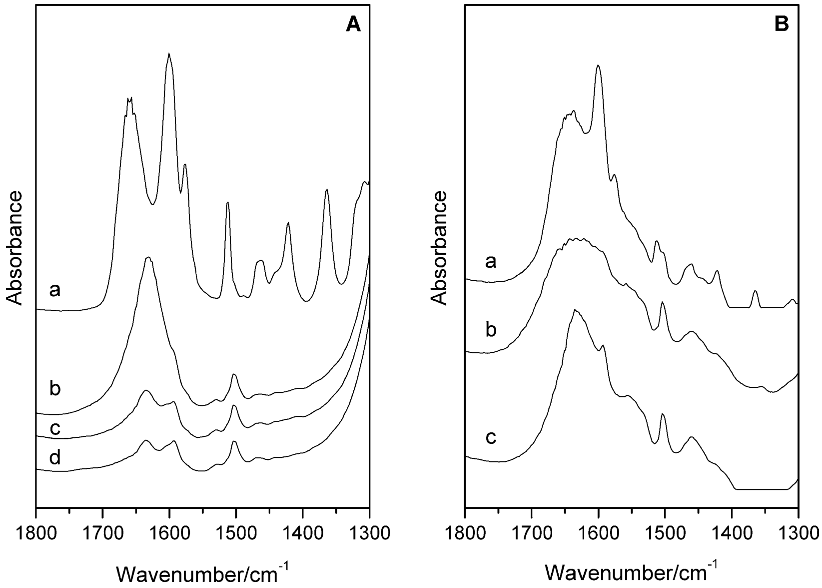

Fig. 5. FTIR spectra of (A) HPA/SiO_2 and (B) HPA/SiZr after (a) acylation of anisole, (b) Soxhlet extraction in CH_2Cl_2, and then evacuation at (c) 298 and (d) 423 K.

atives and condensation products of the reaction product *p*-methoxyacetophenone [9]. The sample HPA/SiZr showed similar spectra to those described for HPA/SiO_2, although additional features at 1556 and 1460 cm^{-1} were observed after Soxhlet extraction (Fig. 5B, b) and after vacuum treatment (Fig. 5B, c). These bands are attributed to the asymmetric and symmetric stretching vibrations of the bidentate acetate species formed by reaction of acetic anhydride or acetic acid with the surface.

The IR spectra of the catalyst after reaction and subsequent treatment to extract the weakly adsorbed products gave evidence for the presence of hydrocarbonaceous species of similar characteristics on both catalysts. In addition to deactivation due to the adsorption of the product *p*-MAP on the acid sites of the catalyst, the contribution from other, undesired products of the reaction might also lead to deactivation of the catalyst.

4. Discussion

Results obtained for the catalysts tested in this work indicate that all the samples are active in the reaction of acylation of anisole with acetic anhydride. However, the differences in the product yields and deactivation trends observed between samples imply an influence of the support, either in the ability to disperse the HPA and subsequently on the distribution and strength of the surface acid sites or in the nature of the sites of the support and the interaction with the adsorbate molecules. Similarities in the calculated molar absorption coefficients for pyridine adsorbed on the HPA on both supports would initially suggest that differences in catalytic behaviour do not originate in different strengths of the Brønsted acid sites.

Characterization of the catalyst by pyridine adsorption by FTIR and TGA reveals differences in the nature and number of the acidic sites for each sample. While the silica is known as a nonacidic support [21], dispersion of the heteropoly acid over its surface results in the generation of a catalyst bearing Brønsted acid properties which are directly related with the heteropoly acid itself. The addition of the heteropoly acid to a support with inherent Lewis and Brønsted acid properties modifies the number and distribution of the acid sites usually by increasing the number and strength of acid sites. These effects depend on the extent of interaction of the HPA with the support. It has been suggested that the interaction of HPA with a SiO_2 surface is much weaker than that for ZrO_2 [22]. This interaction is attributed to the formation of $(\equiv SiOH_2{}^+)(H_2PW_{12}O_{40}{}^-)$ species for SiO_2 [4]. Similar species are assumed to exist for ZrO_2, although, depending on the degree of dehydroxylation, species such as $(\equiv ZrO)_n$–$(H_{3-n}PW_{12}O_{40-n})$ or $(\equiv Zr^+)_n(H_{3-n}PW_{12}O_{40})$ cannot be ruled out [22]. No direct evidence of the type of interaction is apparent here; however, the equivalent values for the molar absorption coefficients for pyridinium on both surfaces could be interpreted as suggesting a degree of similarity in the nature of the supported HPA. The band due to free hydroxyl groups is detected for all the samples evacuated at 523 K, and the only difference is that the feature at 3600 cm^{-1} is better defined for the HPA-containing samples. However, the low loading of the catalyst and the lack of FTIR evidence for HPA species are consistent with the HPA being highly dispersed with the species stabilised by strong interaction with the support.

The proposed mechanism for the acylation reaction implies the formation of an adsorbed acylium ion by interaction of the acylating agent with a Brønsted acid site [23,24]. In the case of the acetic anhydride, the formation of the acylium ion-like species would be linked to the production of acetic acid:

$$(CH_3CO)_2 + H^+OZ^- \rightarrow CH_3CO^+\cdots OZ^- + CH_3COOH. \tag{1}$$

The acetic acid formed may be molecularly adsorbed at an H-bond donor ($OH^{\delta+}$) or acceptor (O^{2-}) site [25]. Alternatively, acetate species, most likely bidentate, can be formed by interaction of acetic acid with Lewis acid–base pairs.

$$CH_3COOH + M^{n+} + O^{2-} \text{ (or } OH^-) \rightarrow CH_3COO^-\cdots M^{n+} + OH^- \text{ (or } H_2O). \tag{2}$$

Identification of the surface species present and their role in reaction should provide insight into the mechanistic details of the reaction. Infrared experiments show that AcAn adsorption occurs readily on HPA/SiO_2, forming primarily hydrogen-bonded species and silyl species due to dissociative adsorption of the molecule. The free OH groups of the silica support seem to be involved in the formation of these species as previously described for the adsorption of acetic acid on silica and on silica-supported catalysts [19,26]. A TPD after AnAc adsorption on a siliceous MCM-41 sample showed that the dominant mode of desorption of AcAn at low temperatures [27] resulted from nondissociative weak interactions of the compound with the surface in contrast with the behaviour observed on zeolites. If acyl species participate in the catalytic cycle, failure to detect these here would account for the lack of catalytic activity. However, the yield to *p*-MAP over HPA/SiO_2 was the highest among the samples tested. It is possible that acyl species are formed but as these are a minority, they may be obscured by the dominant silyl species. It is also possible that not all the sites detected by pyridine adsorption are accessible to the reactant molecules if it is considered that the reaction occurs on the external surface. Since the HPA may absorb pyridine into its bulk, an overestimation of the number of active sites would be estimated by this method.

FTIR spectra after anisole and AnAc coadsorption for HPA/SiZr reveal that in addition to molecularly adsorbed acetic acid, acetate and acyl species are formed. The acyl species are formed by reaction with Brønsted acid sites. The acetate species can be formed by adsorption of either the AcAn or the acetic acid produced as a by-product of the AcAn adsorption at the Brønsted sites. This process requires the existence of Lewis acid (M^{n+}) and base (O^{2-}, OH^{-}) sites. Acetate species are highly thermally stable and are still detected on the catalyst after reaction and after the chemical extraction procedure (Fig. 5B). Similar results were found for sulfated zirconia catalysts studied in acylation reactions using different acylating agents [28].

FTIR spectra after reaction confirm the adsorption of products (Figs. 5A(a) and 5B(a)) and formation of residues on both HPA/SiO_2 and HPA/SiZr. The greater density of strong Brønsted acid sites as determined by pyridine on HPA/SiZr, and thus with the ability to form active acyl species, contrasts with the lower yields obtained for this catalyst. This could imply that not all the sites capable of protonating the base are active in reaction due to differences in strength as a consequence of the interaction of the HPA with the support. However, it is plausible to suspect that the lower yield originates from the greater extent of deactivation for SiZr and HPA/SiZr samples. One possibility could involve residual acetate species which block sites which otherwise provide access for anisole to the active catalyst sites. The absence of appropriate sites on the silica support prevents the formation of such species.

Deactivation during acylation reactions is generally attributed to reversible and irreversible effects [9]. The former is associated with strong product adsorption while the latter is mainly related to coke deposition on the active sites. The role of product inhibition has been confirmed for zeolites and heteropolyacid/SiO_2 catalysts by applying a Langmuir–Hinshelwood model to calculate the adsorption equilibrium constants of reactants and product [13,29,30]. Although competitive adsorption between anisole and acetic anhydride exists [30], product inhibition was the most dominant factor affecting the reaction with an adsorption coefficient ratio, $K_{\text{product}}/K_{\text{acetic anhydride}}$ of 11.80 at 363 K for p-methylacetophenone on HBEA [30], and $K_{\text{product}}/K_{\text{anisole}}$ was 37 at the same temperature for HPA/SiO_2 [13]. Addition of MAP to the reaction mixture decreased the yield due to deactivation of the HPA/SiO_2 while addition of the acetic acid by-product had no effect on the yield [13]. Using a similar methodology [29,30], $K_{\text{product}}/K_{\text{anisole}}$ at 363 K for catalysts here was 23, 93, and 146 for HPA/SiO_2, SiZr, and HPA/SiZr, respectively. This order is qualitatively consistent with the ranking of catalysts in terms of overall product yields and therefore consistent with a deactivation due to inhibition by strong product adsorption.

It should be noted that acetic acid is a poorer acylating agent than the corresponding anhydride since acylium ion-like species are only formed to a limited extent from acetic acid on silica-supported heteropoly acid catalyst [31]. Also, as observed for HPA/SiO_2 catalysts here, surface acetates are not formed over such a catalyst, and consequently no influence is observed by the addition of acetic acid to the reaction mixture.

Optimisation of these catalysts involves a balance between yield and deactivation. In terms of deactivation for supported HPA catalysts, apart from the role of product adsorption and coke deposition, the influence of the support on acid properties and how these modify catalyst behaviour should be considered. A high density of strong acid sites, with adjacent Brønsted acid and Lewis acid–base pair centres, appears to be detrimental, reducing the yield and enhancing deactivation due to strong product adsorption. Higher yields and greater deactivation resistance are obtained with systems presenting only strong Brønsted acid sites.

5. Conclusions

HPA/SiO_2–ZrO_2, SiO_2–ZrO_2, and HPA/SiO_2 were all active in the acylation of anisole using acetic anhydride, although the activity did not respond to the number of Brønsted acid sites present for each sample. Failure to link activity and number of Brønsted acid sites arose due to differences in the rates of deactivation suffered by each catalyst which appeared to depend on the relative strengths of adsorption of the reaction product. The extents of deactivation differed for each of the samples, although the SiO_2–ZrO_2 and the HPA/SiO_2–ZrO_2 showed very similar behaviour. The choice of an inert support was beneficial in terms of reducing the extent of deactivation process.

Acknowledgments

We thank Mrs. C. Wain and Dr. I. Mohmand for obtaining some of the experimental data.

References

[1] G.A. Olah, Friedel–Crafts and Related Reactions, Wiley–Interscience, New York, 1973.

[2] S. Goto, M. Goto, Y. Kimura, React. Kinet. Catal. Lett. 41 (1990) 27.

[3] K. Arata, M. Hino, Appl. Catal. 59 (1990) 197.

[4] I.V. Kozhevnikov, Chem. Rev. 98 (1998) 171.

[5] C. Trolliet, G. Coudurier, J.C. Vedrine, Top. Catal. 15 (2001) 73.

[6] G.I. Kapustin, T.R. Brueva, A.L. Klyachko, M.N. Timofeeva, S.M. Kulikov, I.V. Kozhevnikov, Kinet. Katal. 31 (1990) 1017.

[7] A. Bielański, A. Lubańska, J. Poźniczek, A. Micek-Ilnicka, Appl. Catal. A 238 (2003) 239.

[8] P. Botella, A. Corma, J.M. López-Nieto, S. Valencia, R. Jacquot, J. Catal. 195 (2000) 161.

[9] D. Rohan, C. Canaff, E. Fromentin, M. Guisnet, J. Catal. 177 (1998) 296.

[10] B. Bachiller-Baeza, J.A. Anderson, J. Catal. 212 (2002) 231.

[11] D.J. Rosenberg, J.A. Anderson, Catal. Lett. 83 (2002) 59.

[12] D.J. Rosenberg, B. Bachiller-Baeza, T.J. Dines, J.A. Anderson, J. Phys. Chem. B 107 (2003) 6526.

[13] J. Kaur, K. Griffin, B. Harrison, I. Kozhevnikov, J. Catal. 208 (2002) 448.

[14] J.A. Anderson, C.A. Fergusson, J. Non-Cryst. Solids 246 (1994) 673.

[15] J.A. Anderson, C. Fergusson, I. Rodríguez-Ramos, A. Guerrero-Ruiz, J. Catal. 192 (2000) 344.

[16] N. Mizuno, M. Misono, Chem. Rev. 98 (1998) 199.
[17] L.A. Gambaro, L.E. Briand, Appl. Catal. A 264 (2004) 151.
[18] D.J. Rosenberg, F. Coloma, J.A. Anderson, J. Catal. 210 (2002) 218.
[19] R.P. Young, Canad. J. Chem. 42 (1969) 2237.
[20] J. Shibata, K. Shimizu, S. Satokawa, A. Satsuma, T. Hattori, Phys. Chem. Chem. Phys. 5 (2003) 2154.
[21] J.A. Anderson, C.H. Rochester, in: A. Hubbard (Ed.), Encyclopaedia of Surface and Colloid Science, Dekker, New York, 2002, p. 2528.
[22] E. López-Salinas, J.G. Hernández-Cortéz, I. Schifter, E. Torres-García, J. Navarrete, A. Gutiérrez-Carrillo, T. López, P.P. Lottici, D. Bersani, Appl. Catal. A 193 (2000) 215.
[23] U. Freese, F. Heinrich, F. Roessner, Catal. Today 49 (1999) 237.
[24] Y. Ma, Q.L. Wang, W. Jiang, B. Zuo, Appl. Catal. A 165 (1997) 199.
[25] D. Jackson, G.J. Kelly, D. Lennon, React. Kinet. Catal. Lett. 70 (2000) 207.
[26] W. Rachmady, M.A. Vannice, J. Catal. 207 (2002) 317.
[27] M.L.M. Bonati, R.W. Joyner, M. Stockenhuber, Catal. Today 81 (2003) 653.
[28] J. Deutsch, A. Trunschke, D. Müller, V. Quaschning, E. Kemnitz, H. Lieske, Catal. Lett. 88 (2003) 9.
[29] E.G. Derouane, C.J. Dillon, D. Bethell, S.B. Derouane-Abd Hamid, J. Catal. 187 (1999) 209.
[30] E.G. Derouane, G. Crehan, C.J. Dillon, D. Bethell, H. He, S.B. Derouane-Abd Hamid, J. Catal. 194 (2000) 410.
[31] L.A.M. Cardoso, W. Alves, A.R.E. Gonzaga, L.M.G. Aguiar, H.M.C. Andrade, J. Mol. Catal. A: Chem. 209 (2004) 189.